

1 **PlasmidEC and gplas2: An optimised short-read approach to**
2 **predict and reconstruct antibiotic resistance plasmids in**
3 ***Escherichia coli***

4 Julian A. Paganini¹, Jesse J. Kerkvliet¹, Lisa Vader¹, Nienke L. Plantinga¹, Rodrigo Meneses¹,
5 Jukka Corander^{2,3,4}, Rob J.L. Willems¹, Sergio Arredondo-Alonso^{2,3*} and Anita C. Schürch^{1*}

6 **Affiliations:**

7 ¹Department of Medical Microbiology, University Medical Center Utrecht, Utrecht, The
8 Netherlands.

9 ²Department of Biostatistics, Faculty of Medicine, University of Oslo, Oslo, Norway.

10 ³Parasites and Microbes, Wellcome Sanger Institute, Cambridge, UK

11 ⁴Helsinki Institute of Information Technology, Department of Mathematics and Statistics,
12 University of Helsinki, Finland

13 * Authors contributed equally.

14 **Corresponding author:**

15 a.c.schurch@umcutrecht.nl

16 **Keywords:**

17 WGS, plasmids, assembly graph, illumina, short reads, antibiotic resistance, bioinformatics,
18 *Escherichia coli*.

19 **Abstract**

20 Accurate reconstruction of *Escherichia coli* antibiotic resistance gene (ARG) plasmids from
21 Illumina sequencing data has proven to be a challenge with current bioinformatic tools. In this
22 work, we present an improved method to reconstruct *E. coli* plasmids using short reads. We
23 developed plasmidEC, an ensemble classifier that identifies plasmid-derived contigs by
24 combining the output of three different binary classification tools. We showed that plasmidEC
25 is especially suited to classify contigs derived from ARG plasmids with a high recall of 0.941.
26 Additionally, we optimised gplas, a graph-based tool that bins plasmid-predicted contigs into
27 distinct plasmid predictions. Gplas2 is more effective at recovering plasmids with large
28 sequencing coverage variations and can be combined with the output of any binary classifier.
29 The combination of plasmidEC with gplas2 showed a high completeness (median=0.818) and
30 F1-score (median=0.812) when reconstructing ARG plasmids and exceeded the binning
31 capacity of the reference-based method MOB-suite. In the absence of long read data, our
32 method offers an excellent alternative to reconstruct ARG plasmids in *E. coli*.

33 Data Summary

34 No new sequencing data have been generated in this study. All genomes used in this research
35 are publicly available at the GenBank and Sequence Read Archive of the National Center for
36 Biotechnology Information. Accession numbers are specified in Supplementary Materials.

37 Scripts to reproduce the results reported in this manuscript can be accessed at
38 <https://gitlab.com/jpaganini/ecoli-binary-classifier>. The ensemble classifier, plasmidEC, is
39 publicly available at <https://gitlab.com/mmb-umcu/plasmidEC> (release 1.3.1), and gplas2
40 (release 1.0.0) can be found at <https://gitlab.com/mmb-umcu/gplas2>.

41 Impact Statement

42 *Escherichia coli* has emerged as a highly pervasive multidrug resistant pathogen on a global
43 scale. The dissemination of resistance is significantly influenced by plasmids, mobile genetic
44 elements that facilitate the transfer of antimicrobial resistance genes within and between diverse
45 bacterial species. Consequently, precise and high-throughput identification of plasmids is
46 imperative for effective genomic surveillance of resistance. However, accurate plasmid
47 reconstruction remains challenging with the use of affordable short-read sequencing data. In
48 this work, we present a novel method to accurately predict and reconstruct *E. coli* plasmids
49 based on Illumina data. Additionally, we demonstrate that our approach outperforms the
50 reference-based method MOB-suite, especially when reconstructing plasmids carrying
51 antimicrobial resistance genes.

52 Introduction

53 *Escherichia coli* is a commensal gram-negative bacterium inhabiting the gastrointestinal tract
54 but is also the leading cause of bloodstream and urinary tract infections in humans [1,2]. In
55 recent years, the emergence and spread of multidrug resistant *E. coli* lineages limits the
56 treatment options for such infections [3,4]. Moreover, a recent assessment of the global burden
57 of antimicrobial resistance (AMR) estimated that AMR *E. coli* infections accounted for more
58 than 250,000 deaths in 2019, placing *E. coli* as one of the most prevalent AMR pathogens
59 worldwide [5].

60 Horizontal gene transfer is one of the main drivers behind the rapid spread of AMR [6–8].
61 Antibiotic resistance genes (ARGs) are commonly associated with mobile genetic elements
62 (MGEs), which facilitate their mobility across bacteria [9,10]. Out of these MGEs, plasmids
63 play a pivotal role by disseminating AMR in clinical settings as well as in other environments
64 [11–13]. Plasmids are frequently transmitted among bacteria of the same species, but they can
65 also be shared between bacteria of different species or even different genera [14–17]. Given
66 their relevance in the spread of AMR genes, it is critical to develop high-throughput methods
67 to identify plasmids in a precise, fast and accessible manner.

68 Bacterial genomes have been massively studied using short-read sequencing platforms.
69 However plasmids tend to contain repetitive elements that cannot be spanned by short-reads
70 and thus their sequence is usually fragmented into several contigs and mingled with other
71 genomic elements. This makes it hard to reconstruct complete plasmids from short-read
72 sequencing data [18].

73 Several fully-automated bioinformatic tools are currently available to predict plasmids from
74 short-read sequencing data. They can be broadly categorised into two groups: (i) tools that
75 produce a binary classification of contigs as either plasmid- or chromosome-derived, predicting
76 the total plasmid content of a bacterial strain, often referred to as the ‘plasmidome’ (without

77 reconstructing individual plasmids), and (ii) tools that aim to recover complete sequences for
78 individual plasmids [19]. The latter group, termed plasmid reconstruction tools, provides a more
79 suitable output for plasmid epidemiology studies.

80 We recently evaluated the performance of several plasmid reconstruction tools for use with *E.*
81 *coli* short-read data [19]. We found that the best performing tool, MOB-suite [20], only
82 achieved the correct reconstruction of 50.2% of the plasmids. Moreover, all tools
83 underperformed when attempting to reconstruct plasmids containing antibiotic resistance genes
84 (ARG-plasmids), ranging from 3.4% to 27.9% correct ARG-plasmid reconstructions. These
85 results emphasised the need to improve current methods to predict ARG-plasmids in *E. coli*.

86 Here, we present a new high-throughput method to reconstruct *E. coli* plasmids from short-read
87 sequencing data. Firstly, we optimised gplas [23], a plasmid binning tool, to compute walks in
88 the assembly graph corresponding to plasmids with a pronounced coverage variation. Secondly,
89 we developed an ensemble classifier, plasmidEC, combining multiple existing binary
90 classification tools (Plascope [21], RFplasmid [22], Platon [23] and mlplasmids [24]) to predict
91 plasmid-derived contigs. Coupling plasmidEC with gplas2 allowed to accurately bin plasmid-
92 derived contigs into separate components corresponding to individual plasmid sequences. Our
93 method outperforms all currently available plasmid reconstruction tools for *E. coli*, especially
94 for predicting ARG-plasmids.

95 **Methods**

96 All scripts used to reproduce the analyses can be found at gitlab.com/jpaganini/ecoli-binary-classifier. R version 3.6.1. was used for all R scripts.

98 *Benchmark datasets*

99 A dataset of 240 complete *E. coli* genomes from 8 different phylogroups and 117 sequence
100 types (STs), carrying 631 plasmids, was selected as previously described in Paganini et al. [19].
101 Samples were isolated from animals, humans and the environment, resulting in a diverse dataset
102 with respect to phylogeny and plasmid content. All genome sequences were completed by the
103 combination of short- and long-read sequencing data. Short-read sequences and complete
104 genomes were downloaded from NCBI using SRA tools (v2.10.9) and ncbi-genome-download
105 (v0.2.10) (<https://github.com/kblin/ncbi-genome-download>), respectively. Genomes present in
106 the training datasets or reference databases of existing plasmid classification tools (mlplasmids,
107 PlaScope, Platon and/or RFPlasmid) were removed (n=26). The remaining 214 samples,
108 carrying 542 plasmids, were used to benchmark the binary classifiers (Supplementary Data 1).
109 From these, 15 genomes (Supplementary Data 2) were randomly selected for optimisation of
110 the gplas algorithm and excluded from later comparisons. The remaining genomes (n=199, 483
111 plasmids) were used to benchmark the plasmid reconstruction methods.

112 **Benchmarking binary classification tools and construction of plasmidEC**

113 *Selection of contigs for benchmarking*

114 Short-read sequences of each sample were assembled with bactofidia (v1.1)
115 (<https://gitlab.com/aschuerch/bactofidia>), a pipeline that relies on SPAdes for genome assembly
116 (v3.11.1)[25]. The resulting contigs (n=18,963) were labelled as chromosome- or plasmid-
117 derived by alignment to their respective complete genomes using QUAST (v5.0.2)[26]. Only
118 contigs larger than 1,000 bp with an alignment of at least 90% the contig length were considered
119 (n=15,020). Of those, contigs aligning to multiple positions in the genome (ambiguously
120 aligned contigs) were included as long as they exclusively aligned to either the chromosome or

121 to plasmids (n=1,236). The same criterion was used for the inclusion of misassembled contigs
122 (n=1,862). In total, the benchmark dataset included 14,746 contigs (Supplementary Figure S1).

123 *Assessment of the individual binary classifiers*

124 Contigs were classified by mlplasmids (v2.1.20), PlaScope (v.1.3.121), Platon (v.1.619) and
125 RFPlasmid (v.0.0.1722). All tools were run using default parameters. We assessed the
126 performance of the four binary classifiers by comparing, for each contig, their prediction to the
127 true class of the contig, as described in the section above. For PlaScope, an ‘unclassified’
128 prediction was handled as a negative prediction. Predictions were categorised into: True
129 Positives (TP, prediction = plasmid, class = plasmid), True Negatives (TN, prediction =
130 chromosome, class = chromosome), False Positives (FP, prediction = plasmid, class =
131 chromosome) and False Negatives (FN, prediction = chromosome, class = plasmid). Global
132 performance of the tools was evaluated with the following metrics:

133
$$Recall(contig) = \frac{TP}{TP + FN}$$

134
$$Precision(contig) = \frac{TP}{TP + FP}$$

135
$$F1\text{-Score}(contig) = 2 \cdot \frac{Recall(contig) \cdot Precision(contig)}{Recall(contig) + Precision(contig)}$$

136 *Assessment of the ensemble classifiers*

137 To improve the predictions obtained by independent tools, we combined their output into
138 distinct ensemble classifiers that implemented a majority voting system. We tested four
139 different combinations of individual classifiers: mlplasmids/PlaScope/Platon,
140 mlplasmids/PlaScope/RFPlasmid, mlplasmids/Platon/RFPlasmid and
141 PlaScope/Platon/RFPlasmid. A final classification of each contig (chromosome or plasmids)
142 was obtained by combining the output of the tools using an R script (provided in the
143 accompanying code repository). The ensemble classifiers were evaluated using the same
144 metrics as described above.

145 *Construction of plasmidEC*

146 The tool consists of a bash wrapper script that automatically installs and runs all required
147 individual classifiers and combines their results with a majority voting system. Based on the
148 performance for *E. coli*, the combination of PlaScope/Platon/RFPlasmid was selected as the
149 default. PlasmidEC is publicly available at <https://gitlab.com/mmb-umcu/plasmidEC>.

150 **Benchmarking plasmid reconstruction tools**

151 *Running plasmid predictions tools*

152 Prior to assembly, Illumina raw reads were trimmed using trim-galore (v0.6.6)
153 (<https://github.com/FelixKrueger/TrimGalore>) to remove bases with a Phred quality score
154 below 20. Unicycler (v0.4.8) [27] was then applied to perform *de novo* assembly with default
155 parameters. Contigs larger than 1,000 bp were used as input for MOB-suite (v3.0.0) [20], while
156 assembly graphs in GFA format served as input for gplas2 (v2.0.0). To run gplas2, nodes from
157 the graph were first classified as plasmid- or chromosome-derived using either plasmidEC or
158 PlaScope; only nodes larger than 1,000 bp were classified. Output from the tools was modified

159 to assign probabilities for the classification of each node, which is required by the gplas
160 algorithm. For PlaScope, discrete probabilities were assigned based on the node classification
161 status; if a node was classified as plasmid, a probability of 1 was assigned, while chromosome-
162 predicted nodes were assigned zero. In the case of unclassified nodes, a probability of 0.5 was
163 assigned. By default, plasmidEC assigns probabilities based on the fraction of tools that agreed
164 on the classification. For example, if two out of three tools agreed in classifying a node as
165 plasmid, a probability of 0.66 is assigned.

166 *Analysis of the plasmid bin composition*

167 To evaluate the bins created by MOB-suite and gplas2, we used QUAST (v5.0.2) [26] to align
168 the contigs of each bin to the respective complete reference genome. We calculated accuracy,
169 completeness and F1-score on the base-pair level, as specified below.

170
$$Accuracy(bp) = \frac{\text{Alignment length against reference plasmid}(bp)}{\text{Total length of predicted bin}(bp)}$$

171
$$Completeness(bp) = \frac{\text{Alignment length against reference plasmid}(bp)}{\text{Total length of reference plasmid}(bp)}$$

172
$$F1\text{-Score}(bp) = 2 \cdot \frac{Accuracy(bp) \cdot Completeness(bp)}{Accuracy(bp) + Completeness(bp)}$$

173 If a bin was composed of contigs derived from different plasmids, then accuracy_(bp),
174 completeness_(bp) and F1-score_(bp) were reported for each plasmid-bin combination.

175 We also evaluated the number of reference plasmids that were detected by each tool. We
176 consider a reference plasmid as detected when at least a single contig of the plasmid was
177 included into the predictions.

178 To determine *combined completeness* for each reference plasmid, all bins generated in an isolate
179 were combined as follows:

180
$$Combined completeness(bp) = \sum_1^n Completeness(bp) \quad n =$$

181
$$Total number of bins that contain contigs aligning the reference plasmid.$$

182 *Antibiotic Resistance Gene (ARG) Prediction*

183 Resistance genes were predicted by running Abricate (v1.0.1) against the Resfinder [28]
184 database (database indexed on 19 April 2020) with reference plasmids as query, using 80% as
185 identity and coverage cut-off. The same software and parameters were used to predict the
186 presence of ARGs in the plasmid-predicted contigs bins generated by each of the plasmid
187 reconstruction tools.

188 *Evaluation of ARGs binning*

189 For bins that carried ARGs, we calculated Recall(ARG) and Precision(ARG) as indicated
190 below.

191

192
$$Recall(ARG) = \frac{Nr. of correctly predicted ARGs \in bin}{Total nr. of ARGs \in reference plasmid}$$

193
$$Precision(ARG) = \frac{\text{Nr.of correctly predicted ARGs} \in \text{bin}}{\text{Total nr.of ARGs} \in \text{bin}}$$

194 *Evaluating unbinned nodes in gplas predictions*

195 Unitigs classified as unbinned by gplas (n=78) were aligned to the corresponding complete
196 reference genome using QUAST (v5.0.2). The results of these alignments were used to
197 determine the origin of the unitig (plasmid or chromosome). For isolates that contained more
198 than one unbinned unitig (n=19), coverage information of all unitigs (bin and unbinned) was
199 extracted from the header of the FASTA files generated after unicycler assembly. From these
200 data, coverage variance for all replicons was calculated and plotted using R (v.3.6.1).

201 *Evaluating the recovered fraction for each reference plasmid*

202 We calculated the maximum completeness(bp) that can be obtained to reconstruct every
203 reference plasmid using short-read sequencing data. Before applying any classification tool, all
204 nodes from the assembly graph were converted to FASTA format using the 'extract' option of
205 gplas2. Nodes smaller than 1,000 bp or smaller than 500 bp were filtered out using seqtk (v1.3)
206 (<https://github.com/lh3/seqtk>), and remaining nodes were aligned to their respective complete
207 reference genomes using QUAST to obtain the completeness(bp) values. The completeness(bp)
208 value was called the *recovered fraction*.

209 *Read coverage of missing reference plasmids*

210 A small number of plasmids were either completely missed or recovered with low completeness
211 after short-read assembly. In order to determine if these sequences were also missing from
212 short-reads, trimmed Illumina reads were aligned to reference genomes using BWA MEM
213 (v.0.7.17) [29] with default parameters. Resulting SAM files were converted to BAM and sorted
214 using SAMtools (v1.9) [30]. Read coverage per base was determined using BEDTOOLS
215 (v2.30.0) [31].

216 **Results**

217 **Optimisation of gplas to improve the reconstruction of *E. coli* plasmids**

218 Gplas is an algorithm that performs *de novo* reconstruction of plasmids through multiple steps
219 (Figure 1 - Steps 1 to 3) [32]. In short, nodes from the assembly graph are initially classified as
220 plasmid-derived or chromosome-derived by an external binary classification software, which
221 also assigns a probability to the classifications. Then, plasmid-predicted unitigs act as seeds to
222 compute plasmid walks with homogeneous coverage in the assembly graph using a greedy
223 approach. Finally, these unitigs are binned together into individual components based on their
224 co-existence in the computed plasmid walks. A detailed description of the algorithm can be
225 found in the original publication [32]. Given that gplas performed sub-optimally when
226 reconstructing *E. coli* plasmids in our previous study [19], in gplas2 we introduced two major
227 modifications to the algorithm:

228 A) Expansion of the input options for binary classification

229 Coupling gplas with an accurate binary classifier improves the reconstruction of plasmids, as
230 we previously demonstrated for *Enterococcus faecalis* and *Klebsiella pneumoniae* [32,33].
231 Consequently, the gplas2 algorithm accepts predictions from any binary classifier, provided
232 they output classification probabilities and expected file formats.

233 B) Re-iterating plasmid walks over initially unbinned contigs

234 Gplas constructs plasmid walks over the assembly graph to connect unitigs that potentially
235 originate from the same plasmid (Figure 1 - Step 2). Consequently, plasmid-predicted unitigs
236 that can't be connected to other unitigs through these walks are classified as unbinned, and are
237 not included in the plasmid predictions (Figure 1 - Step 3). Unbinned unitigs seem to originate
238 from reference plasmids that were sequenced with a pronounced coverage variation
239 (Supplementary Figure S2). This sequencing artefact poses a challenge to the gplas algorithm,
240 which builds plasmid walks from unitigs with homogeneous coverage. Consequently, we
241 modified gplas to consider these coverage variations (Figure 1 - Steps 4 & 5). Whenever
242 unbinned unitigs are produced, gplas2 will generate a second round of binning in bold mode by
243 running two additional steps:

244 1) *Computation of plasmid walks in bold mode starting from unbinned unitigs*

245 If unbinned unitigs are predicted, new bold plasmid walks will be constructed. When creating
246 the bold walks, a higher coverage variance threshold between plasmid-predicted unitigs is
247 allowed. This threshold can be defined by the user and is a multiple of the coverage variance
248 observed for chromosome-predicted unitigs. Only bold plasmid walks that start from unbinned
249 unitigs will be retained to use in the next step, while the rest will be discarded (Figure 1 - Step
250 4).

251 2) *Plasmidome network reconstruction and repartitioning*

252 Plasmid walks produced during bold mode are merged with plasmid walks from normal mode.
253 Based on these combined data, plasmidome networks are reconstructed and repartitioned
254 (Figure 1 - Step 5) to create new bins, using the same algorithms as in step 3.

255 We optimised the predictions obtained with gplas2 using a subset of 15 *E. coli* genomes that
256 contained unbinned unitigs and that were excluded from subsequent benchmarking efforts
257 (Supplementary Data 2). For bold walks, we allowed a coverage variance of 5, 10, 15 or 20
258 times the coverage variance observed for the chromosome-predicted unitigs. Plasmid
259 predictions made with gplas2 exhibited consistently higher completeness(bp) values when
260 compared to the original predictions (Supplementary Figure S3 A). Surprisingly, altering the
261 coverage variance threshold above 5 did not impact completeness(bp) values. In contrast,
262 accuracy(bp) values decreased when allowing a higher coverage variance. The highest F1-
263 Score(bp) values (median=0.78, IQR=0.47 - 0.96) were obtained when using a coverage
264 variance threshold of 5. Consequently, 5 was defined as the default value to construct bold
265 plasmid walks. As a single example, we display the plasmid predictions obtained with and
266 without running bold mode for genome GCA_01382335.1_ASM1382333v1 (Supplementary
267 Figure S3 B and S3 C). In this case, the bold walks allowed to recover 7 additional contigs
268 belonging to plasmids CP057179.1 and CP057180.1.

269 Gplas2, including the aforementioned features and a detailed user guide, can be found at
270 <https://gitlab.com/mmb-umcu/gplas2>.

271 **Comparing binary classification methods for *E. coli***

272 In order to combine gplas2 with the best available binary classifier for *E. coli*, we compared the
273 performance of four different tools (PlaScope, RFPlasmid, mlplasmids and Platon). The
274 benchmark dataset consisted of 14,746 contigs. Of these contigs, 87.3% (n=12,872) were
275 chromosome-derived and 12.7% (n=1,874) were plasmid-derived, as determined by alignment

276 to complete reference genomes.

277 We evaluated the number of contigs which were correctly and incorrectly classified by each of
278 the tools and calculated $\text{recall}_{(\text{contig})}$, $\text{precision}_{(\text{contig})}$ and $\text{F1-score}_{(\text{contig})}$ (Supplementary Table
279 S1). Plascope was able to correctly identify the highest number of plasmid-derived contigs
280 (True Positives, $n=1,629$), while the rest of the tools detected between 1,297 and 1,523 plasmid-
281 derived contigs. Notably, PlaScope also included the least chromosomal contamination in its
282 predictions (False Positives, $n=117$), closely followed by Platon ($n=122$). In contrast,
283 mlplasmids and RFPlasmid included a higher amount of chromosome-derived contigs in their
284 plasmidome predictions ($n=418$ and $n=420$, respectively). PlaScope was the tool with the
285 highest $\text{F1-score}_{(\text{contig})}$ (0.900) followed by Platon (0.861), RFPlasmids (0.798) and mlplasmids
286 (0.722). For most tools, $\text{precision}_{(\text{contig})}$ values were higher than $\text{recall}_{(\text{contig})}$ values, indicating
287 that the predicted plasmidome mostly consists of true plasmid-derived contigs, but also that
288 plasmid contigs were frequently missed by the tools.

289 We also explored the congruence in contig classifications across tools (Figure 2). All tools
290 agreed on the correct classification of 51.8% of plasmid-derived contigs (True Positives: $n=971$,
291 Figure 2A), and another 26.5% plasmid-derived contigs were correctly classified by at least
292 three tools ($n=497$). Also, a high fraction (94.1%) of chromosome-derived contigs were
293 correctly classified by all tools (True Negatives: $n=12,116$, Figure 2B). Moreover, only a
294 minority of plasmid-derived and chromosome-derived contigs were missed by most of the tools
295 and correctly classified by just a single tool (True Positives: 85/1,874, 4.7%, True Negatives:
296 58/12,872, 0.5% respectively). From these observations, we concluded that contig
297 misclassifications are primarily derived from individual tools (Figure 2C and 2D).

298 **PlasmidEC: A voting classifier for improved detection of ARG-plasmid contigs in *E. coli*.**

299 We theorised that discarding software-specific misclassifications, while keeping correct
300 classifications shared by multiple tools, could improve the overall binary classification of *E.*
301 *coli* contigs as plasmid- or chromosome-derived. To explore this, we combined the predictions
302 of three individual classifiers and extracted their majority vote as the final classification.

303 After testing all possible combinations of individual classifiers, we found that
304 Platon/PlaScope/RFPlasmid displayed the highest overall performance of voting classifiers
305 with the highest $\text{F1-score}_{(\text{contig})}$ (0.904). This ensemble classifier achieved an $\text{F1-score}_{(\text{contig})}$
306 similar to PlaScope (0.900) but had a slightly higher $\text{recall}_{(\text{contig})}$ (0.884 and 0.869, respectively)
307 (Figure 3 A and B, Supplementary Table S1).

308 Next, we evaluated $\text{recall}_{(\text{contig})}$ values for a subset of plasmids ($n=114$) encoding antibiotic
309 resistance genes (ARG-plasmids) (Figure 3C and 3D, Supplementary Table S2). This dataset
310 consisted of 860 plasmid-derived contigs, derived from 91 *E. coli* genomes. The $\text{recall}_{(\text{contig})}$ of
311 individual tools ranged from 0.723 (mlplasmids) to 0.884 (PlaScope), whereas the different
312 combinations of tools in a voting classifier reached $\text{recall}_{(\text{contig})}$ values ranging from 0.883
313 (mlplasmids/Platon/RFPlasmid) to 0.941 (Platon/PlaScope/RFPlasmid).

314 Based on these results, the combination of Platon/PlaScope/RFPlasmid was selected as the
315 ensemble classifier to be implemented in a novel tool termed plasmidEC, which is publicly
316 available at <https://gitlab.com/mmb-umcu/plasmidEC>.

317 We measured the computational resources used by the ensemble and individual classifiers
318 (Supplementary Figure S4). Binary classifiers showed considerable differences in both CPU

319 time and memory usage. The average CPU time required per sample was lowest for PlaScope
320 (0.2 mins) and highest for Platon (14.9 mins). Platon also used the largest amount of memory
321 per sample (20.6 Mb). The least amount of memory was required by mlplasmids (2.7 Mb).
322 Because plasmidEC includes the execution of three binary classifiers, time and memory
323 requirements were high, especially when Platon was run. The combination of
324 mlplasmids/PlaScope/RFPlasmid required the least number of resources (CPU time = 4.5 mins,
325 memory = 9.0 Mb) and PlaScope/Platon/RFPlasmid the most (CPU time = 21.5 mins, memory
326 = 21.4 Mb).

327 **Exploiting the information from the assembly graph improves correct binning of ARG
328 plasmids**

329 To reconstruct individual *E. coli* plasmids, gplas2 was combined with plasmidEC and PlaScope,
330 and performance was compared against MOB-suite, which was the best-performing plasmid
331 reconstruction tool for *E. coli* in our recent benchmark study [19]. To retain comparability with
332 the aforementioned study, we started with the same dataset and removed 26 genomes that were
333 present in the PlaScope database and 15 genomes that were used to improve the gplas2
334 algorithm. Consequently, our benchmark dataset consisted of 199 complete *E. coli* genomes,
335 which carried 483 plasmids. A total of 213 (44.1%) plasmids were classified as small plasmids
336 (smaller than 18,000 bp), while the remaining 270 (55.9%) were large plasmids [19]. Given
337 our interest in predicting ARG-plasmids, and the fact that most ARGs are encoded on large
338 plasmids (n=382/387, 98.7%), we analysed performance separately for large ARG-plasmids
339 (n=96) and large non-ARG-plasmids (n=174).

340 When evaluating the reconstruction of ARG-plasmids, we found that the F1-Score_(bp) values of
341 gplas2 combined with either plasmidEC (gplas2_plasmidEC) or PlaScope (gplas2_PlScope)
342 were similar (Figure 4A, Table 1). However, gplas2_plasmidEC (median=0.81, IQR=0.53 -
343 0.93) performed slightly better than gplas2_PlScope (median=0.76, IQR=0.52 - 0.94).
344 Notably, both gplas2 methods outperformed MOB-suite, which presented a lower F1-Score_(bp)
345 (median= 0.44, IQR= 0.18 - 0.87). As accuracy_(bp) values were nearly identical across tools, the
346 disparity in F1-Scores_(bp) can be explained due to the differences in completeness_(bp). In contrast,
347 combined completeness_(bp) distributions were virtually identical among tools. These results
348 suggested that all methods had a similar capacity to detect contigs derived from ARG-plasmids,
349 but gplas2 performed better at binning these contigs together into individual predictions. This
350 hypothesis was confirmed by analysing the number of bins into which each reference plasmids
351 was fragmented (Figure 4B). For ARG plasmids, we found that MOB-suite fragmented 49% of
352 plasmids into multiple predictions, while both gplas2 methods did so in only 14% of the cases.

353 All tools identified a similar number of plasmid-derived ARGs (Figure 4C). MOB-suite and
354 gplas2_plasmidEC detected 331 (86.6%) ARGs and gplas2_PlScope 327 (85.6%). Moreover,
355 all tools successfully detected all ARGs present in small plasmids (n=5, 100%). In concordance
356 with previous results, recall_(ARG) values (Figure 4D) for gplas2 predictions were higher than
357 those obtained with MOB-suite (Table 1). This indicates that gplas2 performs better at correctly
358 binning ARGs together into the same bin. However, plasmid predictions made with gplas2 also
359 included a higher number of chromosome-derived ARGs (Figure 4C, Table 1).

360 Interestingly, tools performed similarly well when evaluating the reconstruction of extended
361 spectrum beta-lactamase (ESBL) plasmids (n=42). MOB-suite reconstructions were
362 characterised by having higher accuracy_(bp) and gplas2 methods reconstructed ESBL-plasmids
363 with higher completeness_(bp) (Supplementary Figure S5A). Despite these differences, all tools
364 exhibited similar F1-Score_(bp) values. Additionally, the number of plasmid-borne ESBL genes

365 detected were almost identical across tools (Supplementary Figure S5B). Nevertheless, gplas2
366 methods performed slightly better at binning ARGs into the same prediction (Supplementary
367 Figure S5C).

368 For small plasmids (n=213), all tools displayed similar performance across the three metrics,
369 obtaining near-perfect reconstructions in all cases, with F1-score_(bp) medians of 1
370 (Supplementary Figure S6A, Table 1). This is likely due to most small plasmids being
371 assembled into a single contig (n=196, 92.0%) (Supplementary Figure S6B), and consequently
372 the identification of these contigs as plasmid-derived generally leads to obtaining high values
373 for all metrics. We therefore evaluated the number of small (and large) plasmids detected by
374 each of the tools (Supplementary Figure S6C, Table 1). Interestingly, gplas2_PlasmidEC detected
375 196 (92.0%) small plasmids, and gplas2_PlasmidEC performed similarly, detecting 184
376 (86.4%). Both gplas2-methods outperformed MOB-suite, which detected 174 (81.79%) small
377 plasmids.

378 Finally, we tested the effect of using different contig size cut-offs for plasmid reconstruction.
379 We found no significant differences in performance of the tools when using 500 bp or 1,000 bp
380 as the minimum contig size. A more detailed description of the results from this analysis can
381 be found in the Supplementary Materials and in Supplementary Figures S7 - S10.

382

Discussion

383 Accurately reconstructing *E. coli* plasmids from Illumina reads has proven to be a challenge,
384 especially in the context of ARG-plasmids. In this work, we developed a new high-throughput
385 method to reconstruct *E. coli* plasmids *de novo* from short-read sequencing data. Our method
386 relies on an accurate identification of plasmid-derived nodes in the assembly graph, followed
387 by the binning of these nodes using sequencing coverage and node connectivity information.
388 We proved that our method outperforms other plasmid prediction tools available for *E. coli*,
389 especially when reconstructing ARG-plasmids.

390 To improve the identification of plasmid-derived contigs, we built plasmidEC, an ensemble
391 classifier that combines predictions from three individual binary classifiers and implements a
392 majority voting system. Voting classifiers have been successfully applied in other fields of
393 biology [35–38], but so far not for the problem of plasmidome identification. PlasmidEC
394 correctly identified a large fraction of contigs derived from ARG-plasmids
395 ($\text{Recall}_{(\text{contig})}=0.941$), and considerably outperformed all individual classifiers. Thus, we believe
396 that plasmidEC will be especially useful for plasmidome research that focuses on antibiotic
397 resistance. Notably, all binary classifiers presented higher $\text{recall}_{(\text{contig})}$ for classifying contigs
398 from ARG plasmids than from non-ARG plasmids, suggesting that these sequences might be
399 overrepresented in reference databases which are directly or indirectly used by all tools.

400 When comparing the performance of the tools using the entire benchmark dataset, we found
401 that plasmidEC and PlaScope performed very similarly in terms of $\text{F1-Score}_{(\text{contig})}$. However,
402 plasmidEC showed a higher $\text{recall}_{(\text{contig})}$ but used more computational resources and took a
403 longer time to complete the predictions. Reference-based methods, like PlaScope, are expected
404 to perform well for species like *E. coli* which are abundant in public databases [39]. Supporting
405 this hypothesis, a recent study by Shaw et al. [40] discovered very few novel plasmid sequences
406 in a dataset that included more than 2,000 plasmids from *Enterobacteriaceae* isolates. PlaScope
407 was built around Centrifuge [41], a metagenomic classifier to predict the origin of contigs based
408 on custom databases. Recently, it was also shown that the usage of Kraken [42], another
409 metagenomic classifier using customised databases, outperformed other binary classifiers in
410 *Klebsiella pneumoniae* [41,43]. It would be interesting to explore how tools perform at
411 classifying contigs from species with a limited number of complete genomes in databases. We
412 speculate that in those cases, plasmidEC, which combines tools with diverse computational
413 approaches, could improve predictions to a larger extent.

414 PlasmidEC could be further optimised by (i) multithreading the predictions of the individual
415 tools, which would reduce the computational time to generate the results, (ii) including the
416 possibility to predict the origin of contigs from other species, as long as those are supported by
417 the binary classifiers, and (iii) improving its accuracy by using weighted votes, where a high
418 confidence prediction will contribute more to the final result than a low confidence prediction.

419 We integrated plasmidEC (and PlaScope) with gplas2 to reconstruct individual *E. coli* plasmids.
420 We then compared the performance of gplas2 combined with those classifiers against MOB-
421 suite. Interestingly, the most pronounced differences in performance were observed when
422 reconstructing ARG-plasmids. Although combined completeness_(bp) values indicated that the
423 three tools identified similar fractions of ARG-plasmids, MOB-suite more frequently
424 fragmented ARG-plasmids into multiple bins, yielding low completeness_(bp) and $\text{F1-Score}_{(\text{bp})}$.
425 In contrast, gplas2 (either with plasmidEC or PlaScope) was more successful at binning together
426 contigs into individual plasmid predictions, thus achieving considerably higher values for the
427 aforementioned metrics. Accuracy_(bp) values for all tools were very similar, indicating a similar

428 degree of chimeric predictions. Interestingly, both gplas2 methods performed similarly to
429 MOB-suite when reconstructing plasmids that carry ESBL genes, which suggests that these
430 plasmids might be overrepresented in the database used by MOB-suite to make predictions.

431 We recently described that ARG plasmids from *E. coli* are particularly difficult to reconstruct
432 from short-read data [18], and we suggested that the modular nature of these plasmids could
433 complicate their reconstruction using strict reference-based methods, such as MOB-suite. The
434 results we obtained here seem to confirm this hypothesis. Additionally, we improved the
435 reconstruction of ARG-plasmids by using coverage and node connectivity information. Yet,
436 our study also proves that enriching the assembly graph with accurate information on the origin
437 of contigs (plasmid/chromosome) is equally important. A previous version of gplas, which used
438 mlplasmids as a binary classifier, performed significantly worse at predicting ARG-plasmids in
439 *E. coli* [19]. Moreover, using a simpler graph-based approach that mainly relies on coverage
440 differences to identify plasmids is also insufficient. This approach, applied by plasmidSPAdes,
441 frequently leads to the inclusion of chromosomal contamination [18,19], due to the low copy
442 number that ARG-plasmids often exhibit.

443 We envision that gplas2 could be combined with different binary classification tools to obtain
444 accurate *de novo* plasmid reconstructions for multiple bacterial species. This means that gplas2
445 could, in theory, also be applied to the reconstruction of plasmids in metagenomic samples.
446 However, since a greater number of plasmid-predicted unitigs is expected on metagenomes, the
447 construction of plasmid walks will probably require parallelization in order to keep the
448 computation time within practical limits.

449 Although our method constitutes a considerable improvement of the reconstruction of ARG-
450 plasmids, some limitations should be noted. First, gplas2 does not include insertion sequences
451 (and other repeated elements) into plasmid predictions. This facilitates the process of finding
452 plasmid walks with homogeneous coverages and simplifies the resulting plasmidome network.
453 However, insertion sequences play an important role in the structure and genomic plasticity of
454 plasmids [44], and they are frequently involved in the mobility of ARGs [9,45,46].
455 Additionally, the localization of these MGEs can influence the expression levels of ARGs
456 [47,48], thereby impacting the resulting resistance phenotypes. Consequently, including IS
457 elements would certainly improve the completeness and relevance of plasmid predictions.
458 Some graph-based plasmid reconstruction methods, like HyAsP [49], include repeated elements
459 into predictions. This tool also constructs plasmid walks, and uses coverage information to
460 predict IS copy numbers, thus allowing the same IS to be present in multiple replicons. In the
461 gplas algorithm, considering repeated elements during the construction of the plasmid walks
462 would lead to more entangled plasmidome networks and would complicate the subsequent
463 partitioning step. As an alternative, we could envision adding labels to unitigs after the binning
464 step, and then implementing a label propagation algorithm on the original assembly graph to
465 determine to which bin the different IS elements belong. A similar approach is implemented by
466 the tool GraphBin2 [50], which refines binning results of metagenomics samples. A second
467 disadvantage of our method is the formation of chimeras, which are bins composed of nodes
468 from distinct replicons. As previously mentioned, accurate identification of plasmid derived
469 nodes reduces the number of chromosome-plasmid chimeras. However, preventing the
470 formation of plasmid-plasmid chimeras is more challenging, especially for isolates carrying
471 multiple large plasmids with similar copy numbers. Separating these chimeras could be possible
472 with the use of a plasmid-backbone reference database.

473 To conclude, in this work we presented a new plasmidome prediction tool, named plasmidEC,
474 and optimised gplas to accurately bin predicted plasmid sequences. Compared to existing binary

475 classifiers, plasmidEC achieves increased recall_(contig), especially for contigs that derive from
476 ARG plasmids. The integration of plasmidEC with gplas2 substantially improved the
477 reconstruction of ARG plasmids in *E. coli*. Our method exceeded the binning capacity of the
478 reference-based method MOB-suite, while retaining similar accuracy_(bp) values. The presented
479 approach constitutes the best alternative to accurately predict and reconstruct ARG plasmids *de*
480 *novo* in the absence of long-read data.

481 **Authors contributions**

482 Conceptualization, J.A.P., A.C.S, S.A.A.; methodology, J.A.P., L.V, J.J.K.,S.A.A.; validation
483 and formal analysis, J.A.P., L.V, J.J.K.; resources, supervision and project administration,
484 A.C.S, S.A.A., R.J.L.W, N.L.P; data curation, J.A.P., L.V, ; writing—original draft
485 preparation, J.A.P.; writing—review and editing, J.A.P., A.C.S., N.L.P.; visualisation, J.A.P.,
486 L.V. All authors have read and agreed to the published version of the manuscript.

487 **Conflicts of interest**

488 The authors declare that there are no conflicts of interest.

489 **Funding Information**

490 This work was partially supported by ZonMW (The Netherlands) [541 003 005 to A.C.S.], the
491 Netherlands Centre of One Health (NCOH Complex systems & metagenomics) and by
492 DiSSeMINATE (LSHM19138). This collaboration project is co-funded by the PPP
493 Allowance made available by Health~Holland, Top Sector Life Sciences & Health, to
494 stimulate public-private partnerships. This work was partially supported by the European
495 Union Horizon 2020 research and innovation programme under the Marie Skłodowska-Curie
496 Actions (grant No. 801,133 to S.A.-A).

497 References

- 498 1. Kern WV, Rieg S. Burden of bacterial bloodstream infection-a brief update on epidemiology and
499 significance of multidrug-resistant pathogens. *Clin Microbiol Infect.* 2020;26: 151–157.
- 500 2. Day MJ, Doumith M, Abernethy J, Hope R, Reynolds R, Wain J, et al. Population structure of
501 *Escherichia coli* causing bacteraemia in the UK and Ireland between 2001 and 2010. *J*
502 *Antimicrob Chemother.* 2016;71: 2139–2142.
- 503 3. Tumbarello M, Sanguinetti M, Montuori E, Trecarichi EM, Posteraro B, Fiori B, et al. Predictors
504 of mortality in patients with bloodstream infections caused by extended-spectrum-beta-
505 lactamase-producing Enterobacteriaceae: importance of inadequate initial antimicrobial
506 treatment. *Antimicrob Agents Chemother.* 2007;51: 1987–1994.
- 507 4. Mediavilla JR, Patrawalla A, Chen L, Chavda KD, Mathema B, Vinnard C, et al. Colistin- and
508 Carbapenem-Resistant *Escherichia coli* Harboring mcr-1 and blaNDM-5, Causing a Complicated
509 Urinary Tract Infection in a Patient from the United States. *MBio.* 2016;7.
510 doi:10.1128/mBio.01191-16
- 511 5. Antimicrobial Resistance Collaborators. Global burden of bacterial antimicrobial resistance in
512 2019: a systematic analysis. *Lancet.* 2022. doi:10.1016/S0140-6736(21)02724-0
- 513 6. Jiang X, Ellabaan MMH, Charusanti P, Munck C, Blin K, Tong Y, et al. Dissemination of
514 antibiotic resistance genes from antibiotic producers to pathogens. *Nat Commun.* 2017;8: 15784.
- 515 7. Lerminiaux NA, Cameron ADS. Horizontal transfer of antibiotic resistance genes in clinical
516 environments. *Can J Microbiol.* 2019;65: 34–44.
- 517 8. McInnes RS, McCallum GE, Lamberte LE, van Schaik W. Horizontal transfer of antibiotic
518 resistance genes in the human gut microbiome. *Curr Opin Microbiol.* 2020;53: 35–43.
- 519 9. Che Y, Yang Y, Xu X, Břinda K, Polz MF, Hanage WP, et al. Conjugative plasmids interact with
520 insertion sequences to shape the horizontal transfer of antimicrobial resistance genes. *Proc Natl*
521 *Acad Sci U S A.* 2021;118. doi:10.1073/pnas.2008731118
- 522 10. Zhang S, Abbas M, Rehman MU, Huang Y, Zhou R, Gong S, et al. Dissemination of antibiotic
523 resistance genes (ARGs) via integrons in *Escherichia coli*: A risk to human health. *Environ*
524 *Pollut.* 2020;266: 115260.
- 525 11. Norman A, Hansen LH, Sørensen SJ. Conjugative plasmids: vessels of the communal gene pool.
526 *Philos Trans R Soc Lond B Biol Sci.* 2009;364: 2275–2289.
- 527 12. Lopatkin AJ, Meredith HR, Srimani JK, Pfeiffer C, Durrett R, You L. Persistence and reversal of
528 plasmid-mediated antibiotic resistance. *Nat Commun.* 2017;8: 1689.
- 529 13. von Wintersdorff CJH, Penders J, van Niekerk JM, Mills ND, Majumder S, van Alphen LB, et al.
530 Dissemination of Antimicrobial Resistance in Microbial Ecosystems through Horizontal Gene
531 Transfer. *Front Microbiol.* 2016;0. doi:10.3389/fmicb.2016.00173
- 532 14. Evans DR, Griffith MP, Sundermann AJ, Shutt KA, Saul MI, Mustapha MM, et al. Systematic
533 detection of horizontal gene transfer across genera among multidrug-resistant bacteria in a single
534 hospital. *eLife.* 2020;9. doi:10.7554/eLife.53886
- 535 15. Bosch T, Lutgens SPM, Hermans MHA, Wever PC, Schneeberger PM, Renders NHM, et al.
536 Outbreak of NDM-1-producing *Klebsiella pneumoniae* in a Dutch hospital, with interspecies
537 transfer of the resistance Plasmid and unexpected occurrence in unrelated health care centers. *J*
538 *Clin Microbiol.* 2017;55: 2380–2390.

539 16. Acman M, van Dorp L, Santini JM, Balloux F. Large-scale network analysis captures biological
540 features of bacterial plasmids. *Nat Commun.* 2020;11: 1–11.

541 17. Redondo-Salvo S, Fernández-López R, Ruiz R, Vielva L, de Toro M, Rocha EPC, et al. Pathways
542 for horizontal gene transfer in bacteria revealed by a global map of their plasmids. *Nat Commun.*
543 2020;11. doi:10.1038/s41467-020-17278-2

544 18. Arredondo-Alonso S, Willems RJ, van Schaik W, Schürch AC. On the (im)possibility of
545 reconstructing plasmids from whole-genome short-read sequencing data. *Microb Genom.* 2017;3:
546 e000128.

547 19. Paganini JA, Plantinga NL, Arredondo-Alonso S, Willems RJL, Schürch AC. Recovering
548 *Escherichia coli* Plasmids in the Absence of Long-Read Sequencing Data. *Microorganisms.*
549 2021;9: 1613.

550 20. Robertson J, Nash JHE. MOB-suite: software tools for clustering, reconstruction and typing of
551 plasmids from draft assemblies. *Microb Genom.* 2018;4. doi:10.1099/mgen.0.000206

552 21. Royer G, Decousser JW, Branger C, Dubois M, Médigue C, Denamur E, et al. PlaScope: a
553 targeted approach to assess the plasmidome from genome assemblies at the species level. *Microb
554 Genom.* 2018;4. doi:10.1099/mgen.0.000211

555 22. van der Graaf-van Bloois L, Wagenaar JA, Zomer AL. RFPlasmid: predicting plasmid sequences
556 from short-read assembly data using machine learning. *Microb Genom.* 2021;7.
557 doi:10.1099/mgen.0.000683

558 23. Schwengers O, Barth P, Falgenhauer L, Hain T, Chakraborty T, Goesmann A. Platon:
559 identification and characterization of bacterial plasmid contigs in short-read draft assemblies
560 exploiting protein sequence-based replicon distribution scores. *Microb Genom.* 2020;6.
561 doi:10.1099/mgen.0.000398

562 24. Arredondo-Alonso S, Rogers MRC, Braat JC, Verschuuren TD, Top J, Corander J, et al.
563 mlplasmids: a user-friendly tool to predict plasmid- and chromosome-derived sequences for
564 single species. *Microb Genom.* 2018;4. doi:10.1099/mgen.0.000224

565 25. Bankevich A, Nurk S, Antipov D, Gurevich AA, Dvorkin M, Kulikov AS, et al. SPAdes: A New
566 Genome Assembly Algorithm and Its Applications to Single-Cell Sequencing. *J Comput Biol.*
567 2012;19: 455.

568 26. Gurevich A, Saveliev V, Vyahhi N, Tesler G. QUAST: quality assessment tool for genome
569 assemblies. *Bioinformatics.* 2013;29: 1072–1075.

570 27. Wick RR, Judd LM, Gorrie CL, Holt KE. Unicycler: Resolving bacterial genome assemblies
571 from short and long sequencing reads. *PLoS Comput Biol.* 2017;13: e1005595.

572 28. Bortolaia V, Kaas RS, Ruppe E, Roberts MC, Schwarz S, Cattoir V, et al. ResFinder 4.0 for
573 predictions of phenotypes from genotypes. *J Antimicrob Chemother.* 2020;75: 3491–3500.

574 29. Li H. Aligning sequence reads, clone sequences and assembly contigs with BWA-MEM. 2013.
575 Available: <http://arxiv.org/abs/1303.3997>

576 30. Li H, Handsaker B, Wysoker A, Fennell T, Ruan J, Homer N, et al. The Sequence
577 Alignment/Map format and SAMtools. *Bioinformatics.* 2009;25: 2078.

578 31. Aaron R, Quinlan IMH. BEDTools: a flexible suite of utilities for comparing genomic features.
579 *Bioinformatics.* 2010;26: 841.

580 32. Arredondo-Alonso S, Bootsma M, Hein Y, Rogers MRC, Corander J, Willems RJL, et al. gplas: a
581 comprehensive tool for plasmid analysis using short-read graphs. *Bioinformatics*. 2020;36: 3874–
582 3876.

583 33. Arredondo-Alonso S, Top J, McNally A, Puranen S, Pesonen M, Pensar J, et al. Plasmids Shaped
584 the Recent Emergence of the Major Nosocomial Pathogen *Enterococcus faecium*. *MBio*.
585 2020;11. doi:10.1128/mBio.03284-19

586 34. Rodríguez-Beltrán J, DelaFuente J, León-Sampedro R, MacLean RC, San Millán Á. Beyond
587 horizontal gene transfer: the role of plasmids in bacterial evolution. *Nat Rev Microbiol*. 2021;19:
588 347–359.

589 35. Li Y, Luo Y. Performance-weighted-voting model: An ensemble machine learning method for
590 cancer type classification using whole-exome sequencing mutation. *Quantitative biology*
591 (Beijing, China). 2020;8. doi:10.1007/s40484-020-0226-1

592 36. Millán AP, Alipour F, Hill KA, Kari L. DeLUCS: Deep learning for unsupervised clustering of
593 DNA sequences. *PLoS One*. 2022;17. doi:10.1371/journal.pone.0261531

594 37. Wattanapornprom W, Thammarongtham C, Hongsthong A, Lertampaiporn S. Ensemble of
595 Multiple Classifiers for Multilabel Classification of Plant Protein Subcellular Localization. *Life*.
596 2021;11. doi:10.3390/life11040293

597 38. Xue T, Zhang S, Qiao H. i6mA-VC: A Multi-Classifier Voting Method for the Computational
598 Identification of DNA N6-methyladenine Sites. *Interdiscip Sci*. 2021;13. doi:10.1007/s12539-
599 021-00429-4

600 39. Douarre P-E, Mallet L, Radomski N, Felten A, Mistou M-Y. Analysis of COMPASS, a New
601 Comprehensive Plasmid Database Revealed Prevalence of Multireplicon and Extensive Diversity
602 of IncF Plasmids. *Front Microbiol*. 2020;0. doi:10.3389/fmicb.2020.00483

603 40. Shaw LP, Chau KK, Kavanagh J, AbuOun M, Stubberfield E, Gweon HS, et al. Niche and local
604 geography shape the pangenome of wastewater- and livestock-associated Enterobacteriaceae. *Sci
605 Adv*. 2021;7. doi:10.1126/sciadv.abe3868

606 41. Kim D, Song L, Breitwieser FP, Salzberg SL. Centrifuge: rapid and sensitive classification of
607 metagenomic sequences. *Genome Res*. 2016 [cited 10 Feb 2022]. doi:10.1101/gr.210641.116

608 42. Wood DE, Lu J, Langmead B. Improved metagenomic analysis with Kraken 2.
609 doi:10.1101/762302

610 43. Gomi R, Wyres KL, Holt KE. Detection of plasmid contigs in draft genome assemblies using
611 customized Kraken databases. *Microbial genomics*. 2021;7. doi:10.1099/mgen.0.000550

612 44. Vandecraen J, Chandler M, Aertsen A, Van Houdt R. The impact of insertion sequences on
613 bacterial genome plasticity and adaptability. *Crit Rev Microbiol*. 2017;43: 709–730.

614 45. Razavi M, Kristiansson E, Flach C-F, Joakim Larsson DG. The Association between Insertion
615 Sequences and Antibiotic Resistance Genes. *mSphere*. 2020;5. doi:10.1128/mSphere.00418-20

616 46. Partridge SR, Kwong SM, Firth N, Jensen SO. Mobile Genetic Elements Associated with
617 Antimicrobial Resistance. *Clin Microbiol Rev*. 2018;31. doi:10.1128/CMR.00088-17

618 47. Kamruzzaman M, Patterson JD, Shoma S, Ginn AN, Partridge SR, Iredell JR. Relative Strengths
619 of Promoters Provided by Common Mobile Genetic Elements Associated with Resistance Gene
620 Expression in Gram-Negative Bacteria. *Antimicrob Agents Chemother*. 2015;59.
621 doi:10.1128/AAC.00420-15

622 48. Turton JF, Ward ME, Woodford N, Kaufmann ME, Pike R, Livermore DM, et al. The role of
623 ISAbal in expression of OXA carbapenemase genes in *Acinetobacter baumannii*. FEMS
624 *Microbiol Lett*. 2006;258. doi:10.1111/j.1574-6968.2006.00195.x

625 49. Müller R, Chauve C. HyAsP, a greedy tool for plasmids identification. *Bioinformatics*. 2019;35:
626 4436–4439.

627 50. Mallawaarachchi VG, Wickramarachchi AS, Lin Y. Improving metagenomic binning results with
628 overlapped bins using assembly graphs. *Algorithms Mol Biol*. 2021;16: 3.

629

630

Figures and Tables

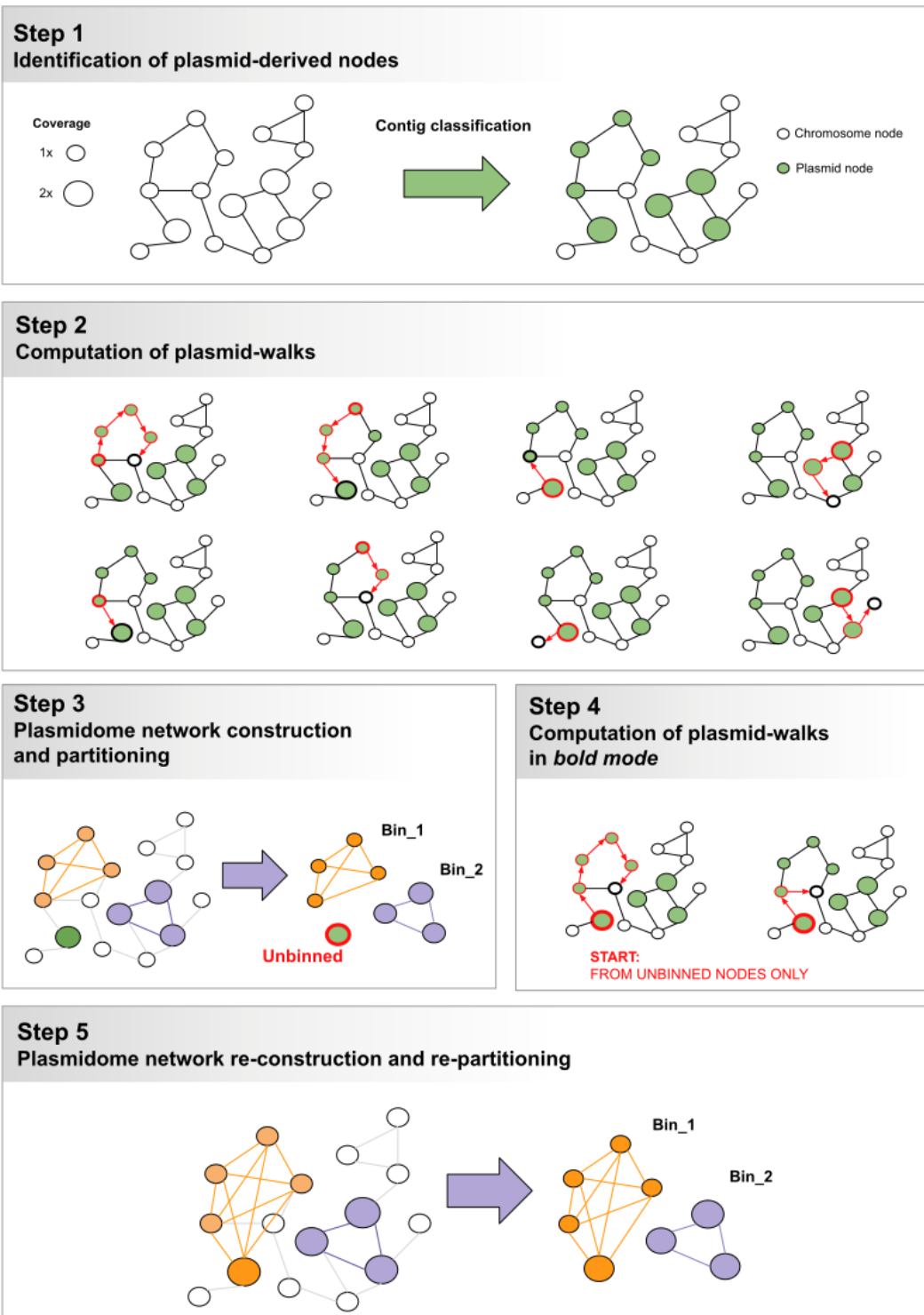
631

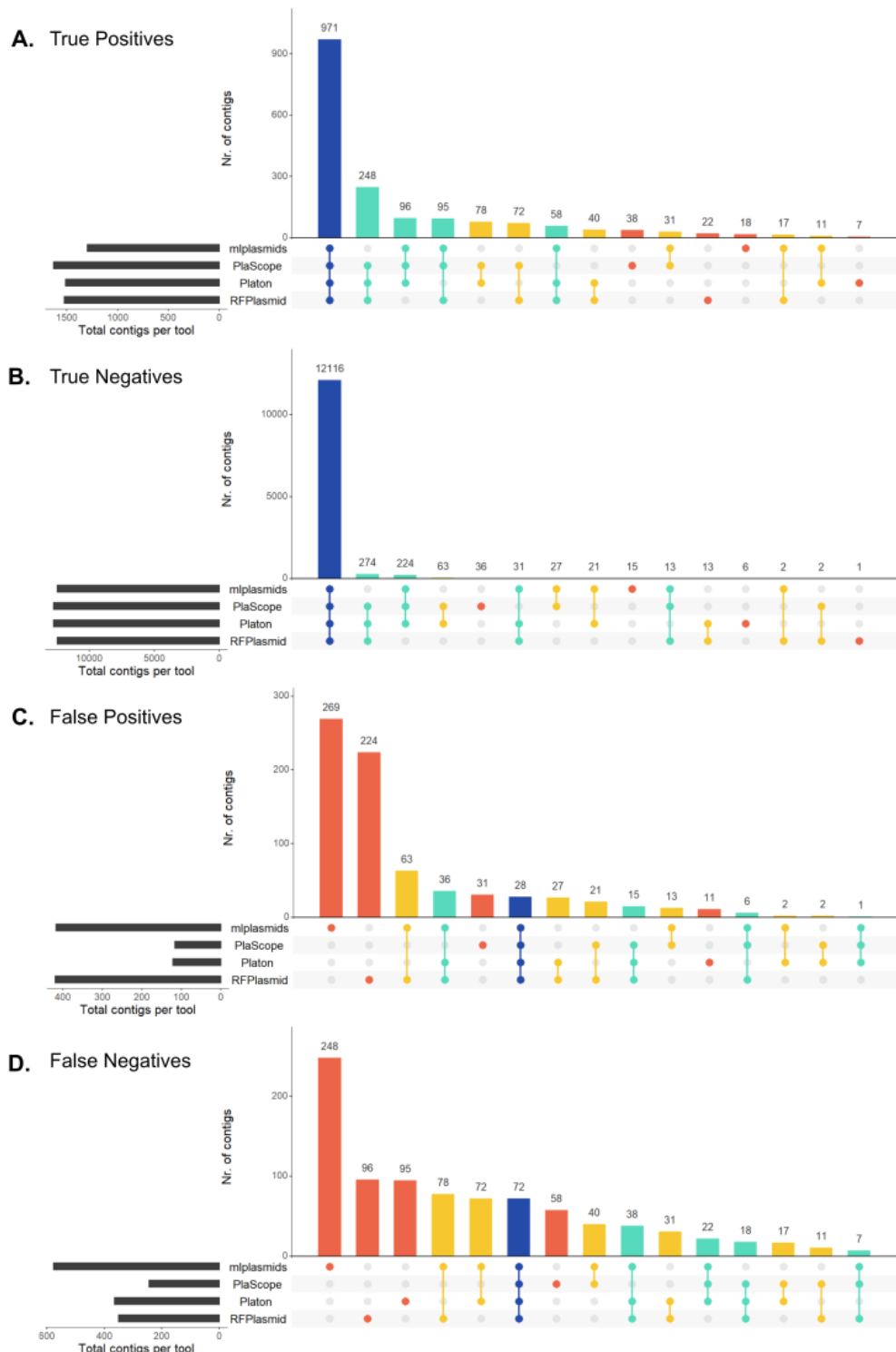
Table 1. Performance summary of three plasmid prediction tools, for the prediction of different plasmid types.

	MOB-suite	gplas2_plasmidEC	gplas2_PlScope
Large Plasmids (n=270)			
Nr. of detected plasmids*	263 (97.4%)	253 (93.7%)	254 (94.1%)
ARG-Plasmids (n=96)			
F1-Score(bp) (median, IQR)	0.421 (0.172 - 0.860)	0.812 (0.529 - 0.934)	0.758 (0.520 - 0.936)
Completeness(bp) (median, IQR)	0.317 (0.114- 0.803)	0.818 (0.520 - 0.924)	0.818 (0.531 - 0.924)
Accuracy(bp) (median, IQR)	0.883 (0.591 - 0.982)	0.979 (0.564 - 1)	0.979 (0.520 - 1)
Nr. plasmid-borne ARGs detected	331 (86.6%)	331 (86.6%)	327 (85.6%)
Nr. chromosome-derived ARGs	64	75	75
Recall (ARG) (median, IQR)	1 (0.42- 1)	1 (0.86- 1)	1 (0.86- 1)
Precision (ARG) (median, IQR)	1 (0.82 - 1)	1 (0.75 - 1)	1 (0.77 - 1)
Non-ARG-Plasmids (n=174)			
F1-Score(bp) (median, IQR)	0.910 (0.378 - 0.977)	0.921 (0.596 - 0.983)	0.912 (0.571 - 0.983)
Completeness(bp) (median, IQR)	0.879 (0.245 - 0.967)	0.915 (0.618 - 0.972)	0.918 (0.614 - 0.972)
Accuracy(bp) (median, IQR)	0.978 (0.904 - 1)	1 (0.958 - 1)	1 (0.796- 1)
Small Plasmids (n=213)			
Nr. of detected plasmids*	174 (81.8%)	184 (86.4%)	196 (92.0%)
F1-Score(bp) (median, IQR)	1 (0.985 - 1)	1 (0.991 - 1)	1 (0.990 - 1)
Completeness(bp) (median, IQR)	1 (0.976 - 1)	1 (0.996 - 1)	1 (0.990 - 1)
Accuracy(bp) (median, IQR)	1 (1- 1)	1 (1- 1)	1 (1- 1)
Nr. plasmid-borne ARGs detected	5 (100%)	5 (100%)	5 (100%)

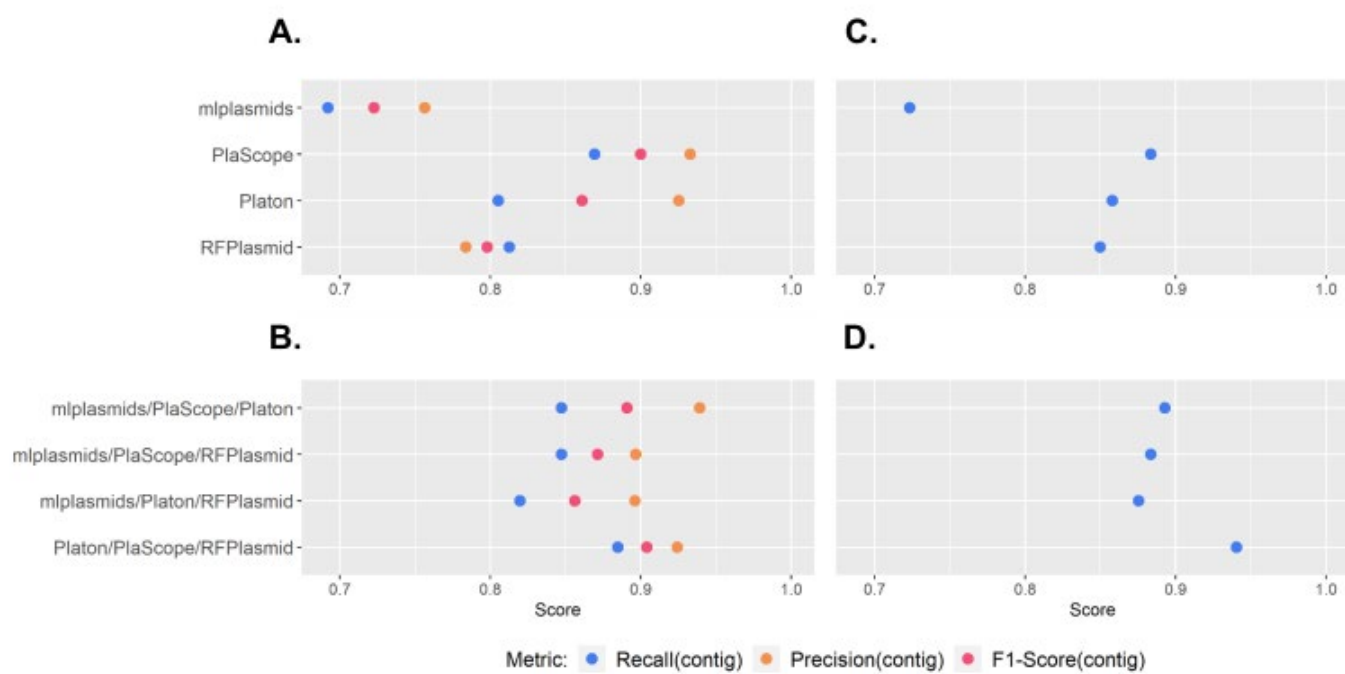
632

*A plasmid is considered detected if at least 1 contig is included in the plasmid predictions

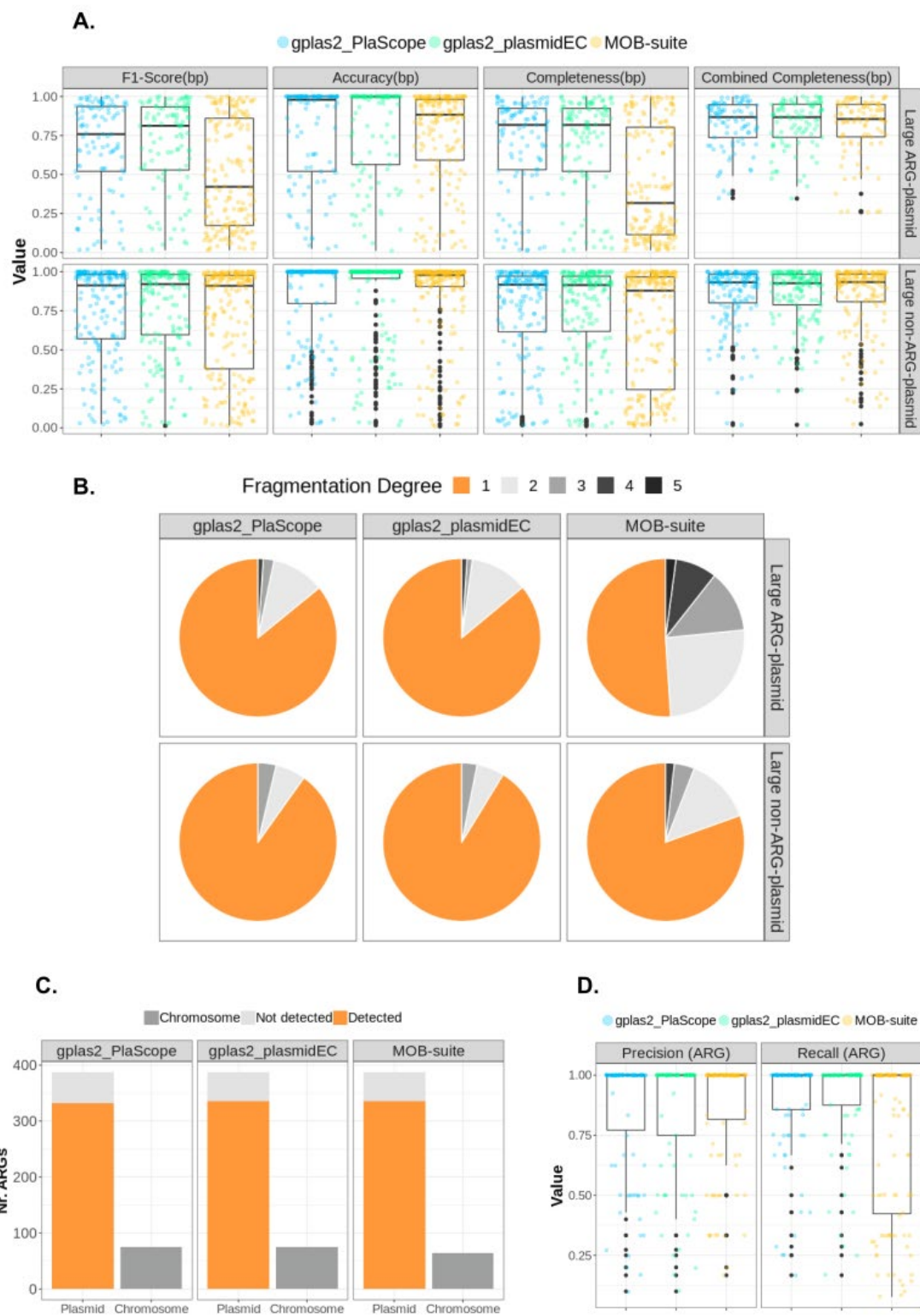




635 **Figure 2.** Upset diagrams showing congruence in contig classification by different binary prediction tools
636 (absolute counts). True Positives (TP; prediction=plasmid, class=plasmid), True Negatives (TN; prediction =
637 chromosome, class=chromosome), False Positives (FP; prediction=plasmid, class=chromosome), False Negatives
638 (FN, prediction=chromosome, class=plasmid). Bar colours indicate the number of tools that concur in the
639 classification of the contigs.



640 **Figure 3.** Performance of individual binary classifiers and plasmidEC combinations, measured by $\text{recall}_{(\text{contig})}$,
641 $\text{precision}_{(\text{contig})}$ and $\text{F1-score}_{(\text{contig})}$ A) Individual classifiers evaluated using full dataset (n=214 genomes). B)
642 PlasmidEC combinations evaluated using full dataset C) Individual classifiers evaluated using a dataset of ARG-
643 plasmids (n=114 plasmids). D) PlasmidEC combinations evaluated using a dataset of ARG-plasmids.



644 **Figure 4.** Benchmarking of plasmid reconstruction methods. A) Recall(bp) , Precision(bp) and
645 precision (bp) values for predictions corresponding to large ARG-plasmids (n=96) and large non-ARG-
646 plasmids (n=174). B) Percentage of reference plasmids that were recovered with different fragmentation
647 degrees (i.e. If contigs belonging to a reference plasmid are assigned to three different predictions, then the fragmentation
648 degree equals three). C) Absolute count of ARGs included (detected) in plasmid predictions, missing ARGs (not
649 detected) and chromosome-derived ARGs incorrectly included (Chromosome). D) Recall(ARG) and
650 Precision(ARG) value.